

AgRISTARS

(E82-10391) SPATIAL AND SPECTRAL SIMULATION
OF LANDSAT IMAGES OF AGRICULTURAL AREAS
(Environmental Research Inst. of Michigan)
29 p HC A03/MF A01 CSCL 02C

N82-32813

Unclas
G3/43 00391

Supporting Research

E82-10391
7. SR-E1-04206
5. NAS9-15476
NASA-CR-167639
A Joint Program for
Agriculture and
Resources Inventory
Surveys Through
Aerospace
Remote Sensing
6. MARCH 1982

TECHNICAL REPORT

SPATIAL AND SPECTRAL SIMULATION OF LANDSAT IMAGES OF AGRICULTURAL AREAS

3 W.F. PONT, Jr.

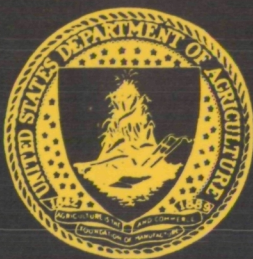
"Made available under NASA sponsorship
in the interest of early and wide dis-
semination of Earth Resources Survey
Program information and without liability
for any use made thereof."

ERIM

A. ENVIRONMENTAL RESEARCH
INSTITUTE OF MICHIGAN
ANN ARBOR, MICHIGAN

UCB

SPACE SCIENCES LABORATORY
UNIVERSITY OF CALIFORNIA
BERKELEY, CALIFORNIA



NASA



NOTICES

Sponsorship. The work reported herein was conducted by the Environmental Research Institute of Michigan under Contract NAS9-15476 for the National Aeronautics and Space Administration, Johnson Space Center, Houston, Texas 77058. I. Dale Browne was Technical Monitor for NASA. Contracts and grants to the Institute for the support of sponsored research are administered through the Office of Contracts Administration.

Disclaimers. This memorandum was prepared as an account of Government sponsored work. Neither the United States, nor the National Aeronautics & Space Administration (NASA), nor any person acting on behalf of NASA:

- (A) Makes any warranty expressed or implied, with respect to the accuracy, completeness, or usefulness of the information, apparatus, method, or process disclosed in this memorandum may not infringe privately owned rights; or
- (B) Assumes any liabilities with respect to the use of, or for damages resulting from the use of any information, apparatus, method, or process disclosed in this memorandum.

As used above, "person acting on behalf of NASA" includes any employee or contractor of NASA, or employee of such contractor, to the extent that such employee or contractor of NASA or employee of such contractor prepares, disseminates, or provides access to any information pursuant to his employment or contract with NASA, or his employment with such contractor.

Availability Notice. Request for copies of this memorandum should be referred to:

National Aeronautics & Space Administration
Scientific & Technical Information Facility
P.O. Box 33
College Park, Maryland 20740

Final Disposition. After this document has served its purpose, it may be destroyed. Please do not return it to the Environmental Research Institute of Michigan.

TECHNICAL REPORT STANDARD TITLE PAGE

1. Report No. SR-E1-04206		2. Government Accession No.		3. Recipient's Catalog No.	
4. Title and Subtitle Spatial and Spectral Simulation of Landsat Images of Agricultural Areas				5. Report Date March 1982	
				6. Performing Organization Code	
7. Author(s) W. F. Pont, Jr.				8. Performing Organization Report No. 152400-18-T	
9. Performing Organization Name and Address Environmental Research Institute of Michigan P.O. Box 8618 Ann Arbor, Michigan 48107				10. Work Unit No.	
				11. Contract or Grant No. NAS9-15476	
				13. Type of Report and Period Covered Technical Report	
12. Sponsoring Agency Name and Address NASA/Johnson Space Center Houston, Texas 77058 Attn: I. D. Browne/SG3				14. Sponsoring Agency Code	
15. Supplementary Notes Dr. Glen Houston/SG3 served as NASA Technical Coordinator of the effort, which was carried out as a part of the Supporting Research Project of the AgRISTARS program.					
16. Abstract A Landsat scene simulation capability was developed. The simulation employs a pattern of ground polygons each with a crop ID, planting date, and scale factor. Historical Greenness/Brightness crop development profiles generate the mean signal values for each polygon. Historical within-field covariances add texture to pixels in each polygon. The planting dates and scale factors create between-field/within-crop variation. Between field and crop variation is achieved by the above and crop profile differences. The Landsat point spread function is used to add correlation between nearby pixels. The next effect of the point spread function is to blur the image. Mixed pixels and misregistration are also simulated. The simulation has been used to study the effects of small fields and misregistration on current Landsat-based crop proportion estimation procedures.					
17. Key Words Landsat, Scene Simulation, Agriculture, Mixtures, Misregistration			18. Distribution Statement		
19. Security Classif. (of this report) Unclassified		20. Security Classif. (of this page) Unclassified		21. No. of Pages xii + 37	22. Price

PRECEDING PAGE BLANK NOT FILMED

SR-E1-04206
NAS9-15476

TECHNICAL REPORT

SPATIAL AND SPECTRAL SIMULATION OF
LANDSAT IMAGES OF AGRICULTURAL AREAS

by

W. F. Pont, Jr.

*Original photography may be purchased
from EROS Data Center
Sioux Falls, SD 57198*

Environmental Research Institute of Michigan
P.O. Box 8618
Ann Arbor, Michigan 48107

March 1982



PREFACE

The Agriculture and Resources Inventory Surveys Through Aerospace Remote Sensing Program, AgRISTARS, is a six-year program of research, development, evaluation, and application of aerospace remote sensing for agricultural resources, which began in Fiscal Year 1980. This program is a cooperative effort of the National Aeronautics and Space Administration, the U.S. Departments of Agriculture, Commerce, and the Interior, and the U.S. Agency for International Development. AgRISTARS consists of eight individual projects.

The work reported herein was sponsored by the Supporting Research (SR) Project under the auspices of the National Aeronautics and Space Administration, NASA. Mr. Robert B. MacDonald, NASA Johnson Space Center, is the NASA Manager of the SR Project and Dr. Glen Houston is the Technical Coordinator for the reported effort.

The Environmental Research Institute of Michigan and the Space Sciences Laboratory of the University of California at Berkeley comprised a consortium having responsibility for development of corn/soybeans area estimation procedures applicable to South America within both the Supporting Research and Foreign Commodity Production Forecasting Projects of AgRISTARS.

This reported research was performed within the Environmental Research Institute of Michigan's Infrared and Optics Division, headed by Richard R. Legault, a Vice-President of ERIM, under the technical direction of Robert Horvath, Program Manager and William A. Malila, Task Leader.

TABLE OF CONTENTS

<u>Section</u>		<u>Page</u>
1	INTRODUCTION	1
2	THE MODEL	3
3	IMPLEMENTATION	9
	3.1 THE FIELD GEOMETRY	9
	3.2 CROP RESPONSE AS A FUNCTION OF TIME AND FIELD . .	10
	3.3 THE CONVOLUTION	11
4	EXAMPLE SIMULATION	13
5	SUMMARY	25
	REFERENCES	27
	DISTRIBUTION LIST	29

PRECEDING PAGE BLANK NOT FILMED

LIST OF ILLUSTRATIONS

<u>Figure</u>		<u>Page</u>
1	Greenness/Brightness Crop Profiles	4
2	Landsat's Point Spread Function	6
3	Landsat Marginal Point Spread Functions	7
4	Field Pattern and Simulated Crops	14
5	Summer Vs. Non-Summer Crops for Day 160	16
6	Corn Vs. Soybeans for Day 160	17
7	Corn Vs. Soybeans for Day 178	18
8	Corn Vs. Soybeans for Day 205	19
9	Corn Vs. Soybeans for Day 223	21
10	Simulated Image for Day 160	22
11	Simulated Image for Day 178	22
12	Simulated Image for Day 205	23
13	Simulated Image for Day 223	23

PRECEDING PAGE BLANK NOT FILMED

LIST OF TABLES

<u>Table</u>		<u>Page</u>
1	Parameters Used in Generating the Simulation	13

PRECEDING PAGE BLANK NOT FILMED

INTRODUCTION

The signal which the Landsat multispectral scanner generates is a function of many variables, few of which we have any control over. The ideal method of understanding a process is to hold all of the variables constant, except those under consideration. This method fails for the most part in the study of the Landsat signal-generation process with its seeming contradiction of vast amounts of data at the pixel level but a scarcity of data with unique combinations of factors such as scan angle, day of year, crop, field pattern, etc. Simulation is a tool which allows one to use combinations of assumed or known effects to infer the composite effect. The uses of a simulation include:

- (1) The study of the interaction of known first order effects;
- (2) Tests of procedures on data generated under known conditions, and
- (3) Empirical estimation of model parameters when fitted to "real data."

The major motivation for the simulation model described here was the need for a capability to investigate, in detail, the effects of various factors on pixel values from small fields, boundaries between fields, and misregistered pixels. Both spectral and spatial properties were of interest. With this model any desired polygonal field pattern can be simulated and spectral-temporal characteristics can differ from field to field, even within a single crop type, and with within-field variances being included.



2

THE MODEL

Consider the point (x,y) on the ground at time t . Except for a set of area zero, (x,y) will be contained in the interior of a field.* Denote this field as k . The main effect which a sensor could detect is that of the crop at point (x,y) . We denote the crop in field k as C_k . We use crop development profiles in Greenness and Brightness to simulate the mean crop response as a function of time since planting. Reference 1 gives the empirically estimated profiles used, while Figure 1 illustrates those for corn, soybeans, small grains, pasture, etc.

Denote the profile for crop c as $P_c(\cdot)$. Note that two fields with the same crop would not in general have the same profile value at time t due to different planting days. Denote the planting date for field k as T_k . The model further assumes that there are field effects beyond crop type and planting date due to soil characteristics, crop variety, fertilizer, etc. These additional between-field, within-crop sources of variability are viewed as geometric noise factors which scale each profile. Denote the scale factor for field k as U_k , where U_k is a random variable with a mean of 1. The profile at (x,y) is:

$$g(x,y,t) := U_k P_{C_k}(t-T_k) + \epsilon_{txy}$$

where ϵ_{txy} is assumed to be a bivariate normal with mean of zero.

The model assumes that the covariance of ϵ_{txy} is a function of crop and time. This is reasonable if the dominant effect in within-field variation is due to crop-field effects. If sensor noise were the real

* e.g., a hedgerow between agricultural fields is, itself, considered to be a field of finite area.

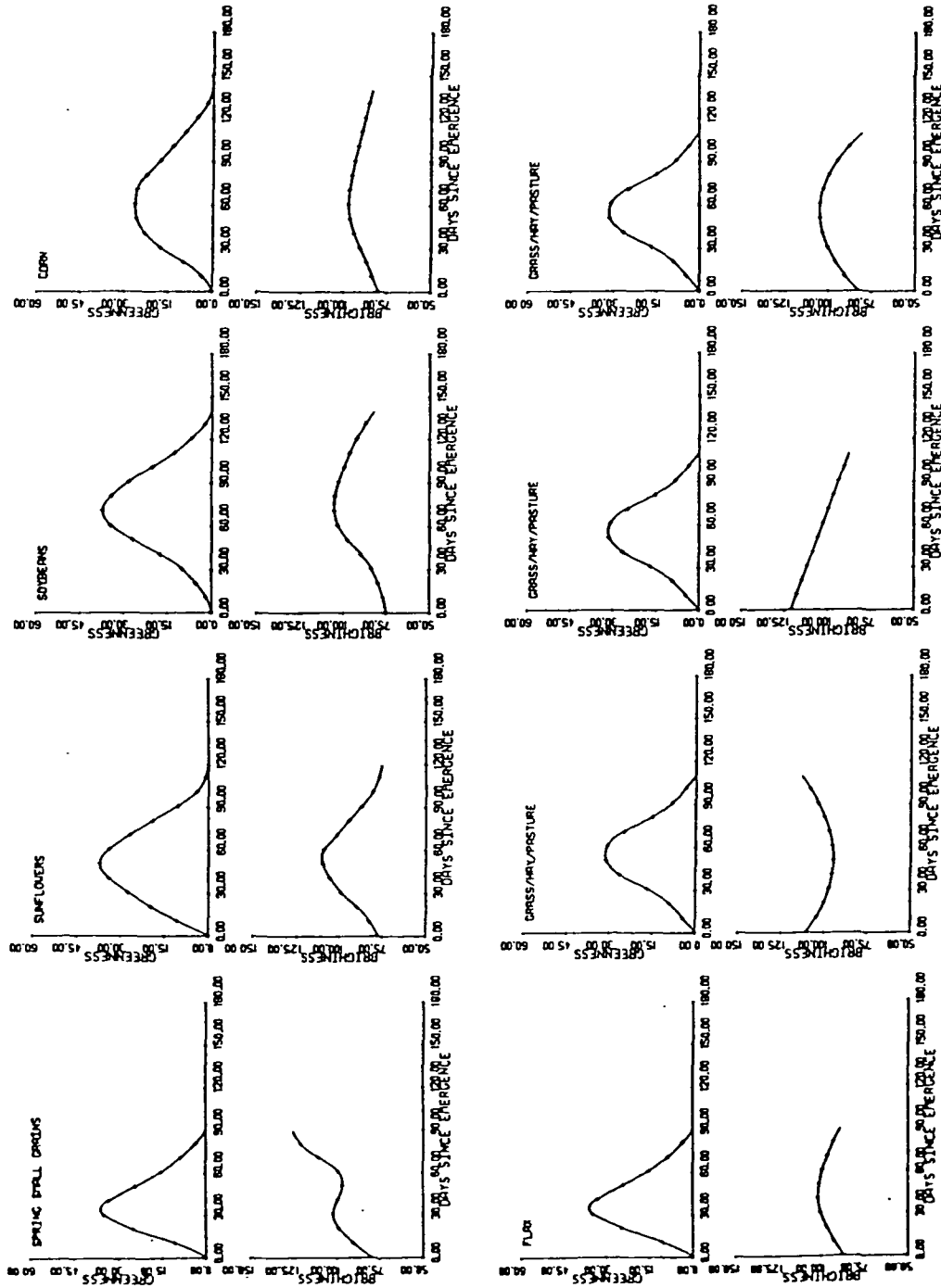


FIGURE 1. GREENNESS/BRIGHTNESS CROP PROFILES

dominant effect, then variances of the Landsat Bands 4, 5, and 6 would be proportional to the signal and the variance would be constant in Band 7.

One of the major problems encountered in multitemporal Landsat data is spatial misregistration between dates. The coordinate system changes between passes of the satellite. The point (x,y) in the satellite's coordinate system does not correspond to the same ground point for different passes. The relationship between ground coordinate system and that of the sensor's is non-linear. There are registration procedures which reduce the differences in coordinate systems; however, there is always a residual error in registration procedures. The model assumes the sensor coordinate system changes only by a translation between passes. If the ground coordinates are (x,y) then the sensor's coordinates at time t are $(x+x_t, y+y_t)$.

This form of misregistration is suitable for most applications using simulation. A more general form of misregistration could be simulated by warping the coordinates which define the fields.

The signal which the sensor receives is not $g(x,y,t)$ but rather

$$f(x,y,t) = \iint g(x+x_t - r, y+y_t - s, t) p(r,s) dr ds$$

where p is the Landsat point spread function.

p was derived in Reference 2 using the sensor's size, blur circle and properties of its three-pole Butterworth filter. Figure 2 gives a three-dimensional drawing of p and Figure 3 gives plots of p along the scan line and along track, at pixel center. The signals which the sensor allows us to observe are:

$$\{f(x + idx, y + jdy, t)\}_{i=1, N_x} \\ j=1, N_y$$

Values for a 5x6-mile AgRISTARS segment are $dx = 79M$, $dy = 57M$, $N_x = 196$, and $N_y = 117$.

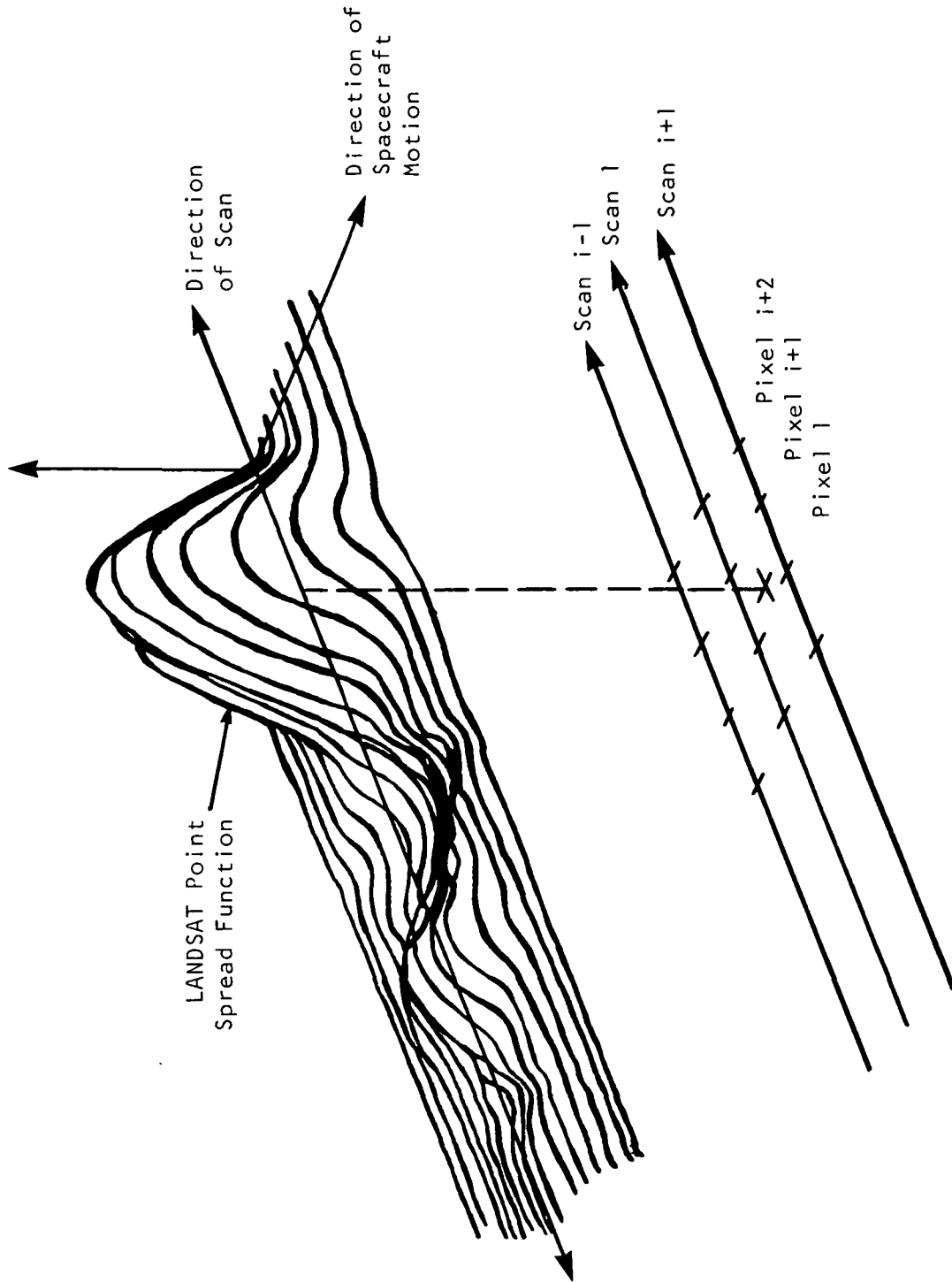
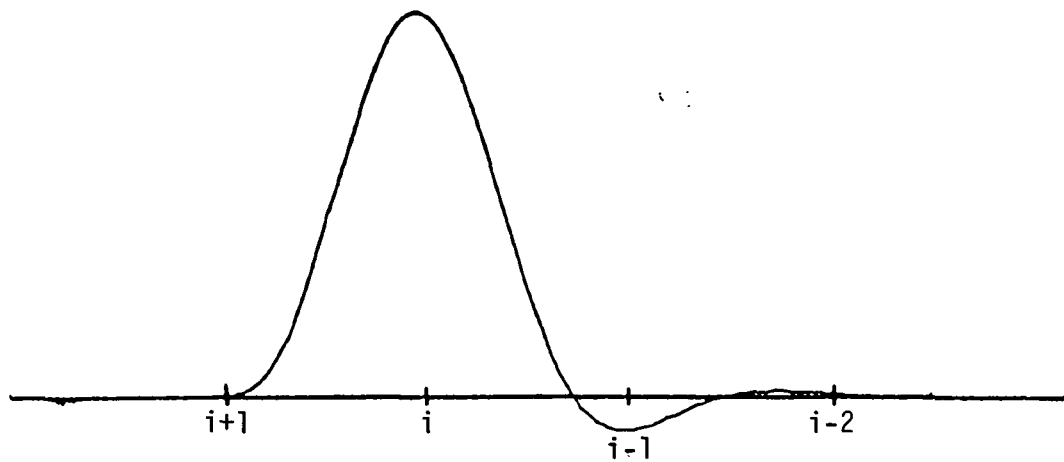
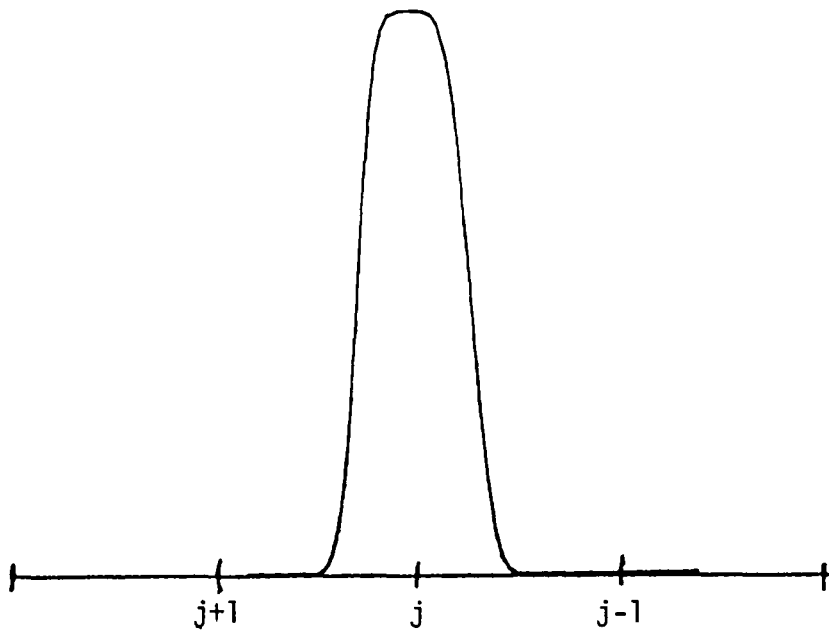


FIGURE 2. LANDSAT'S POINT SPREAD FUNCTION



(a) Landsat Along Scan Line Point Spread Function



(b) Landsat Along Track Point Spread Function

FIGURE 3. LANDSAT MARGINAL POINT SPREAD FUNCTIONS

IMPLEMENTATION

3.1 THE FIELD GEOMETRY

Each field is stored in the computer as a polygon. The vertices of all of the fields are contained in arrays, say $\{U_{kj}, V_{kj}\}$. Polygon (field) k is defined by the vertices k_1, k_2, \dots, k_{N_k} , such that the points $\{U_{kj}, V_{kj}\}_{j=1, N_k}$ circumscribe field k in a counterclockwise direction. It is important that there be no gaps in adjacent fields and non-nil intersections can cause unexpected results. We assume that all fields are simply connected, but more general sets could be incorporated into the model easily.

A two-dimensional grid of points is assigned polygon identification. The point (x,y) is assigned to the first polygon whose winding number is positive. We view these points as subpixels. The polygon search begins with the polygon which contained the previous pixel. If only translation misregistration is to be simulated then this subpixel-to-field assignment only has to be performed once. If more general misregistration is to be simulated then the points $\{U_i, V_i\}$ can be replaced by $\{H_t(U_i, V_i)\}$ where H_t is the warping transform for time t . Examples of H_t are:

$$H_t(U, V) = \left(\sum_{q=0}^5 \sum_{j=0}^q a_{qj} U^j V^{q-j}, \sum_{q=0}^5 \sum_{j=0}^q b_{qj} U^j V^{q-j} \right) \quad (1)$$

and

$$H_t(Z) = A_t(Z - Z_t) + Z_t$$

where

$$Z = u + vi, Z_t = u_t + v_t i, \text{ and } A_t = R_t e^{i\theta_t} \quad (2)$$

Functions of the form (1) are often used to correct geometric distortions in Landsat data (see Reference 3). Regression methods are often used to estimate the coefficients a_{qj} 's and b_{qj} 's. Since there are 21 terms in each coordinate of (1) there should be somewhat more than 21 control points used in the estimation, if estimates of all coefficients are desired. Stepwise regression methods tend to good results with 5-9 control points. Functions of the form (2) represent a rotation of θ_t and a scaling by R_t about (u_t, v_t) .

3.2 CROP RESPONSE AS A FUNCTION OF TIME AND FIELD

The crop for point (x,y) on the ground at time t is:

$$g(x,y,t) = U_k P_{ck}(t-T_k) + \epsilon_{txy}$$

where

- k is the field containing (x,y) ,
- U_k is the scale factor for field k ,
- C_k is the crop growing in field k ,
- T_k is the time of planting,
- $P_c(.)$ is the Greenness/Brightness response of crop c as function of time since planting, and
- ϵ_{txy} is the within-field noise.

The polygon specific parameters U_k , C_k and T_k are saved in a file until all acquisitions are generated. U_k and T_k are viewed as a random variables such that $E\{U_k\} = 1$ and the distribution of T_k is obtained from a crop calendar specific to the region being simulated. Empirical profiles were incorporated for grain, sunflower, corn, soybeans, and three types of grass/pasture/hay. New profiles can be added or old ones modified easily.



Presently the within-field error term is used only to add texture to the pixels contained in a given field. Data which would support an accurate estimation of the covariance matrix of ϵ_{txy} do not exist. The reason is that ground truth polygons often contain more than one field with the same ground truth code, while the field-finding algorithms are constrained to construct field-like regions with small within-field variances.

3.3 THE CONVOLUTION

The convolution of the sensor's point spread function blurs the image by adding correlations between nearby pixels. The sensor's response at point (x,y) and at time t is:

$$f(x,y,t) = \iint g(x-r,y-s,t)p(r,s)drds.$$

We use two different levels of approximations of $f(x,y,t)$:

$$f_1(x,y,t) = \sum_{i=-16}^{48} \sum_{j=-16}^{16} g(x - \frac{i}{16}, y - \frac{j}{16}, t)p_1(\frac{i}{16}, \frac{j}{16})$$

where

$$p_1(\frac{i}{16}, \frac{j}{16}) = \frac{p(\frac{i}{16}, \frac{j}{16})}{\sum_{r=-16}^{48} \sum_{s=-16}^{16} p(\frac{i}{16}, \frac{j}{16})};$$

and

$$f_2(x,y,t) = \sum_{i=-4}^{16} \sum_{j=-4}^4 g(x - \frac{i}{4}, y - \frac{j}{4}, t)p_2(\frac{i}{4}, \frac{j}{4})$$

where

$$p_2(\frac{i}{4}, \frac{j}{4}) = \frac{p(\frac{i}{4}, \frac{j}{4})}{\sum_{r=-4}^{16} \sum_{s=-4}^4 p(\frac{r}{4}, \frac{s}{4})}.$$

EXAMPLE SIMULATION

To illustrate the capabilities of the model, the field pattern from the southwest quarter of Segment 844, during the year 1978, was digitized in polygonal form. Crops were assigned to the fields at random. The crop probability and planting date distributions in Table 1 were used. The field scale factor was generated randomly from the uniform (.95,1.05) distribution for each field. Figure 4 gives a plot of the field pattern used in this simulation. This region was represented by a 256x256 subpixel grid. Each pixel was defined to be a 4x4 subpixel region. The crop signatures were generated at the subpixel level; thus, within-pixel mixture were in multiples of 1/16. The field identification of each point in the subpixel grid was obtained from the polygons. A 64x64 simulated image was produced for the following dates: 160, 169, 178, 187, 196, 205, 214, 223, 232, 241, 250, 259, 268, 277, and 286 with no misregistration. As illustrated in the following discussion, these simulations exhibit spectral, temporal, and spatial characteristics which we have come to associate with real data.

TABLE 1. PARAMETERS USED IN GENERATING THE SIMULATION

<u>Crop</u>	<u>P</u>	<u>T_k Distribution</u>
Grain	.10	N(105,10)
Pasture V1	.05	N(105,10)
Pasture V2	.05	N(105,10)
Pasture V4	.10	N(105,10)
Sunflower	.10	N(138,10)
Corn	.25	N(148,10)
Soybeans	.25	N(156,10)
Flax	.10	N(105,10)

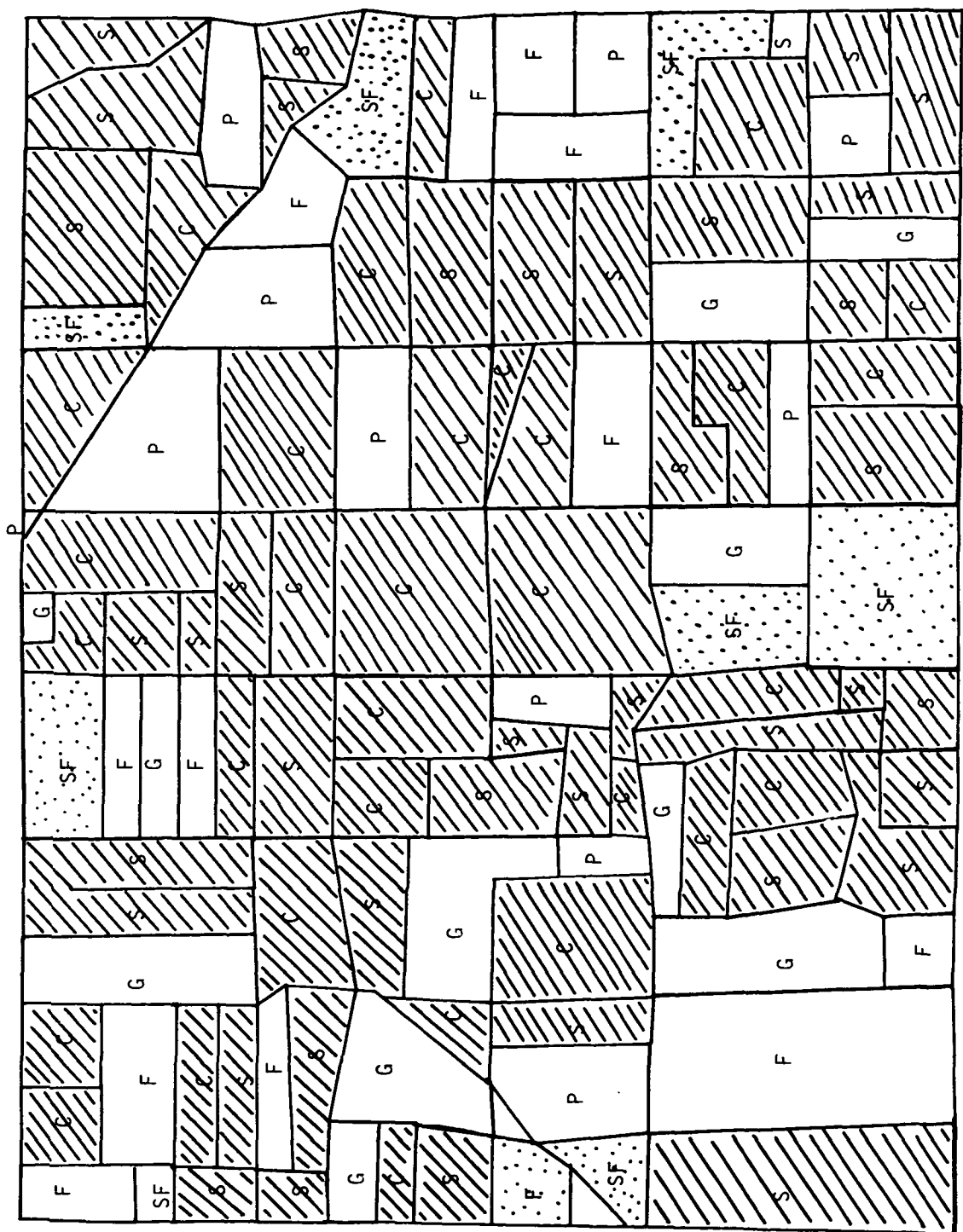


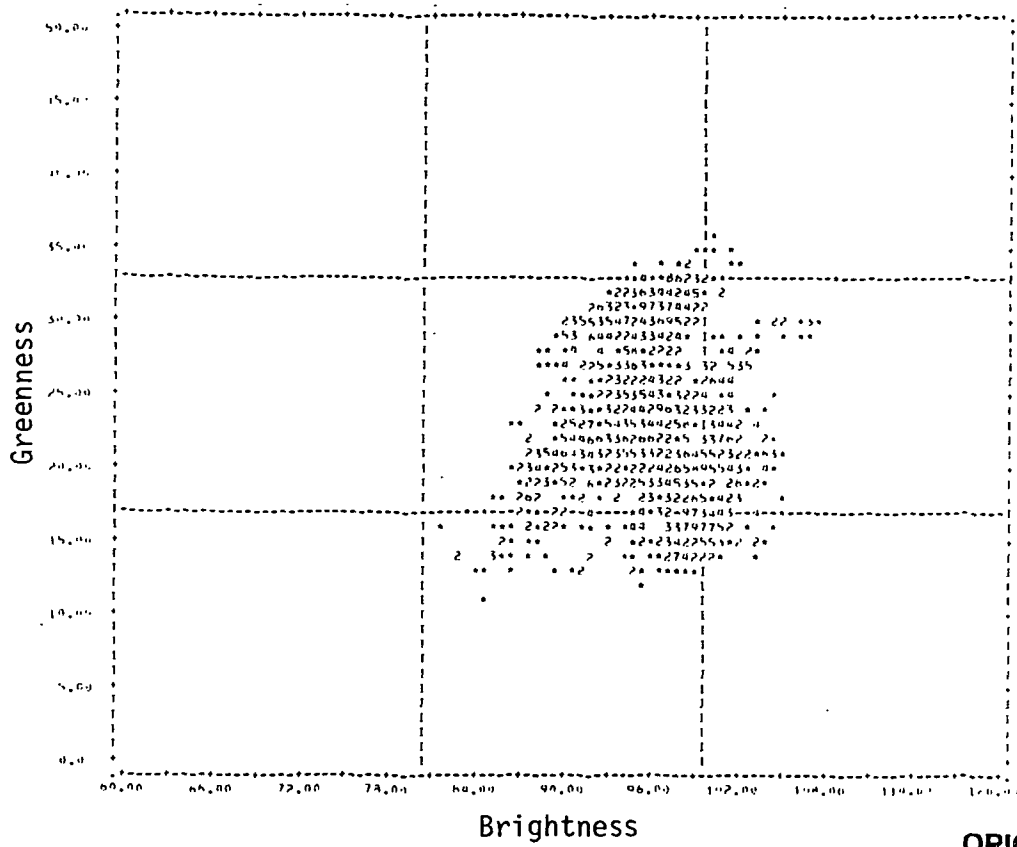
FIGURE 4. FIELD PATTERN AND SIMULATED CROPS

Figures 5(a) and 5(b) give Brightness/Greenness scatterplots for pure non-summer crop and pure summer crop pixels respectively for day of year 160. The vast majority of the pure non-summer crop is above 15 while all of the summer crop is below 15. This example simulation is somewhat unrealistic since 100% of the scene is agricultural. Thus in this simulation one must first separate summer from non-summer crops and then corn from soybeans. At a pixel level we obtain 98% correct classification of summer vs. non-summer crops, using the $G=14$ decision line. On the field level we obtain 100% correct classification because the field geometry allows averaging which reduces variation.

Figures 6(a) and 6(b) give the Greenness/Brightness scatterplots for pure corn and soybean pixels respectively for day of year 160. The mean planting date of corn is 8 days before soybeans in this simulation, see Table 1, thus corn is ahead of soybeans in emergence. This is represented by the higher Greenness values for corn compared to soybeans.

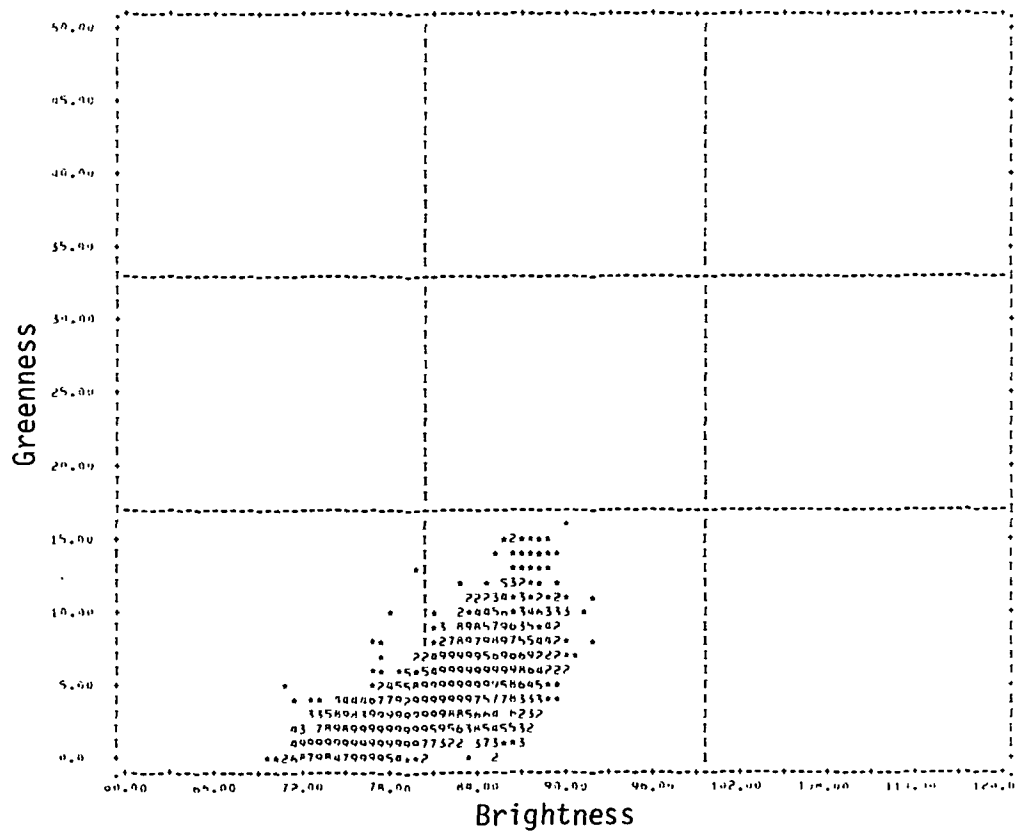
Figures 7(a) and 7(b) give the scatterplots for pure corn and soybeans pixels respectively for day of year 178. The corn tends to have a higher Greenness value than soybeans. Corn and soybeans are separable to the extent that 80% correct classification is possible at the pixel level using a $G=12$ decision line. Better separation can be obtained at the field level.

Figures 8(a) and 8(b) give the pure corn and soybeans Greenness/Brightness scatterplots for day of year 205. Most of the corn has obtained their state of peak Greenness 20 to 30. The soybeans are for the most part still greening up. About 30% of the soybeans are greener than the greenest corn field and about 20% have Greenness values less than the darkest corn field. Classification using the dates 160, 178 and 205 gives an overestimation of corn by 10%.



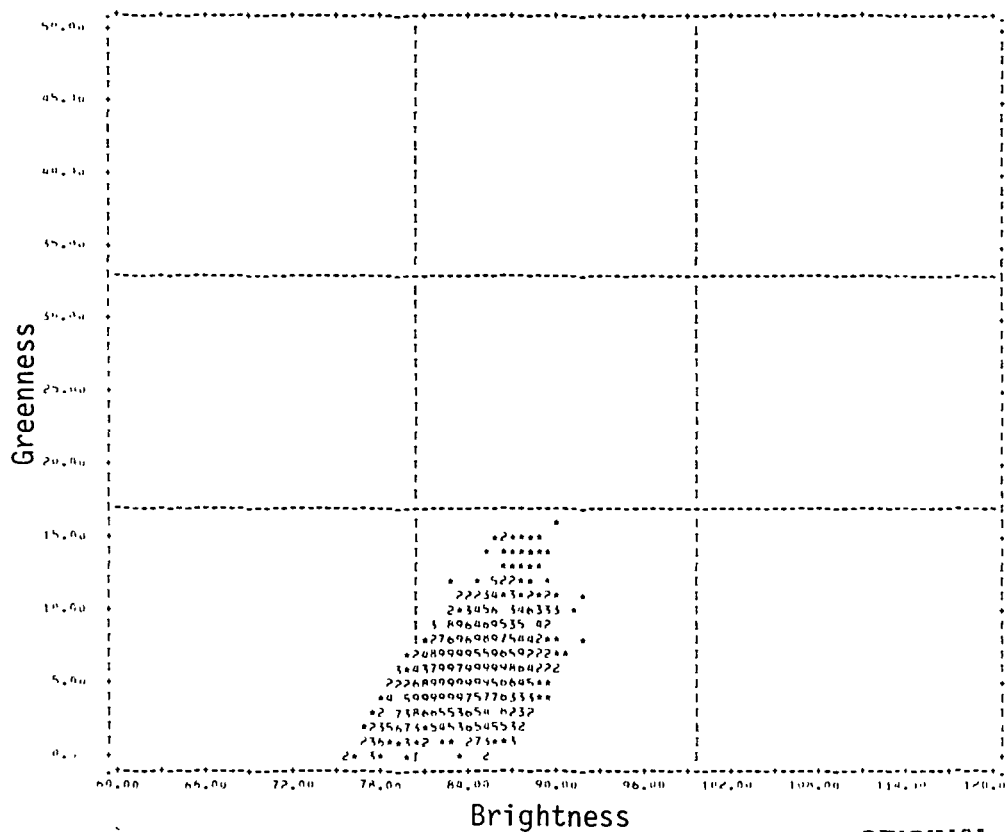
(a) All Pure Non-Summer Crop Pixels

ORIGINAL PAGE IS
OF POOR QUALITY



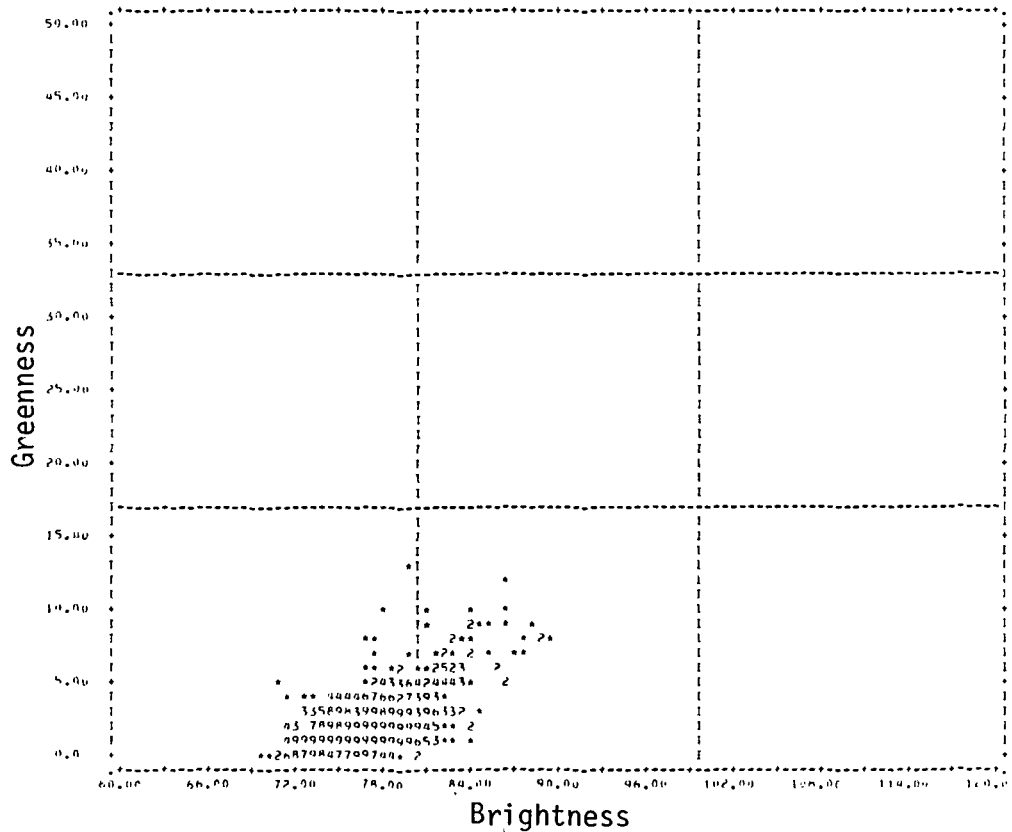
(b) All Pure Summer Crop Pixels

FIGURE 5. SUMMER VS. NON-SUMMER CROPS FOR DAY 160



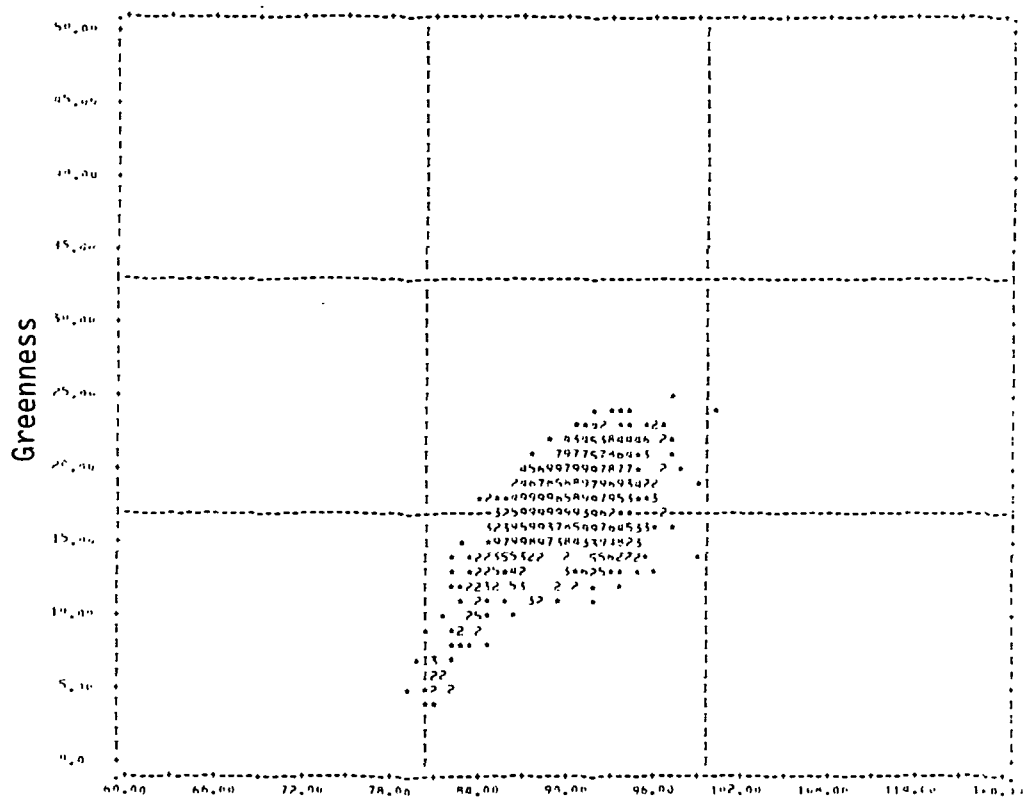
(a) Pure Corn Pixels

ORIGINAL PAGE IS
OF POOR QUALITY



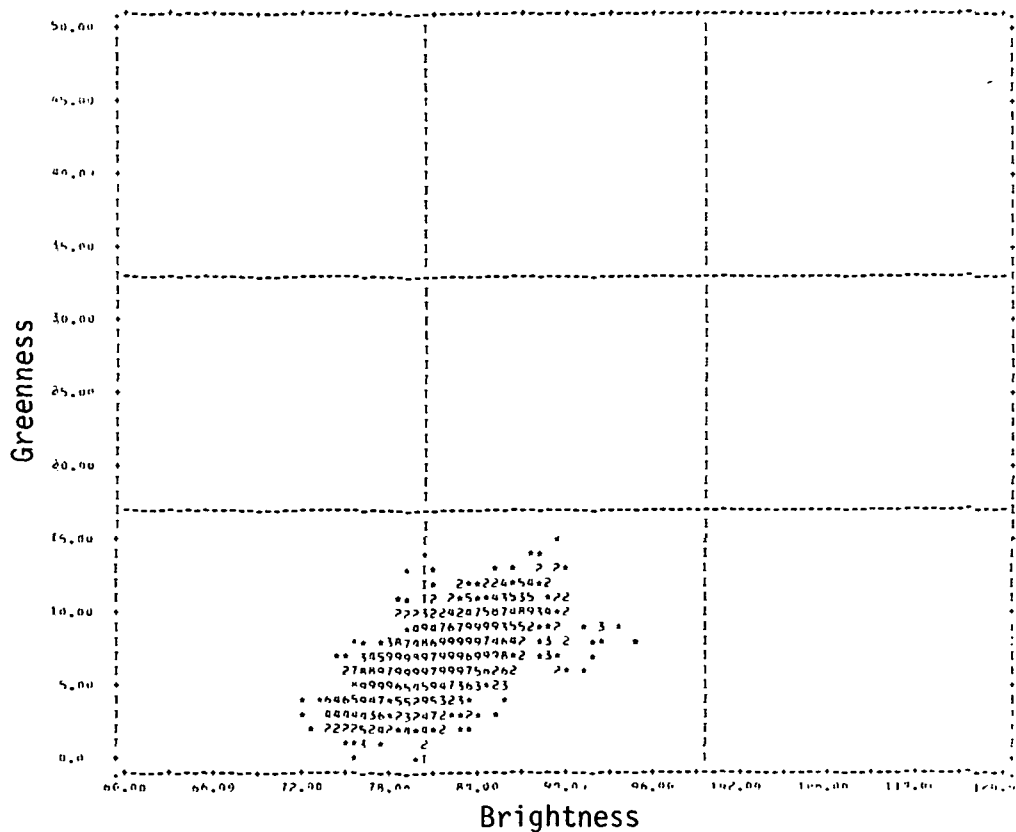
(b) Pure Soybeans Pixels

FIGURE 6. CORN VS. SOYBEANS FOR DAY 160



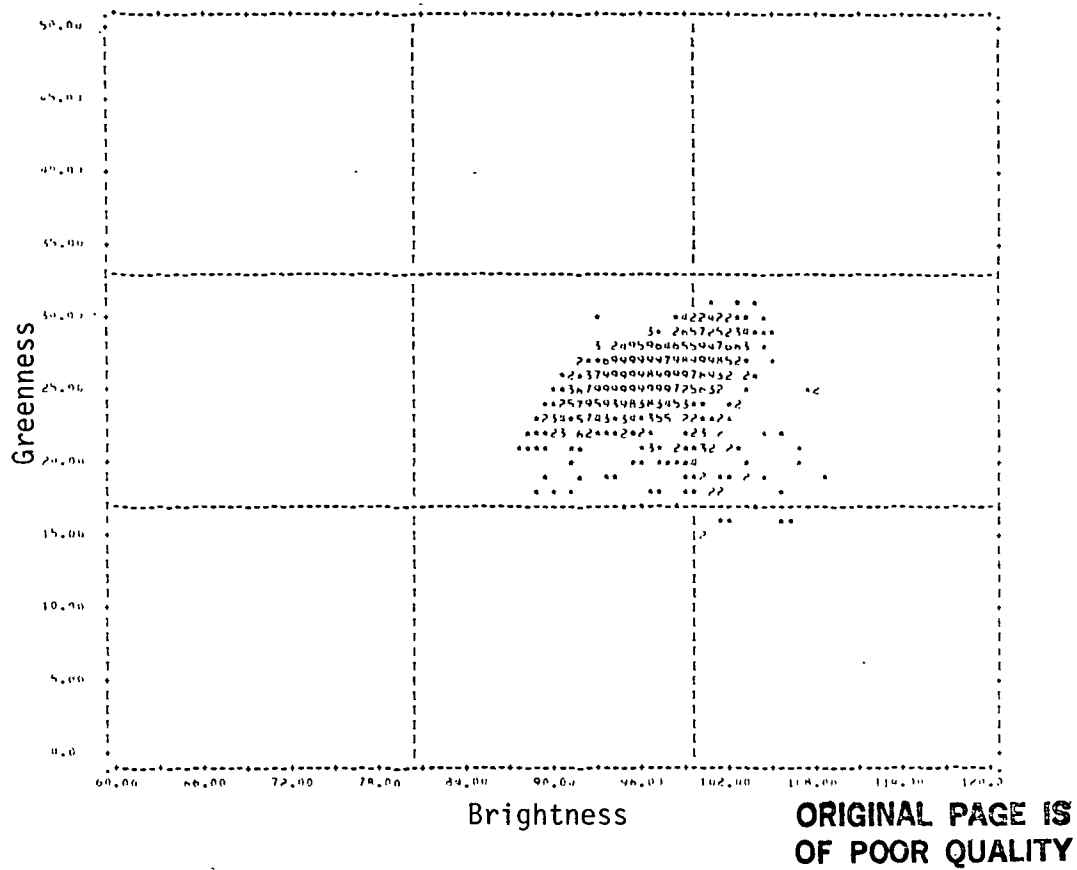
**ORIGINAL PAGE IS
OF POOR QUALITY**

(a) Pure Corn Pixels

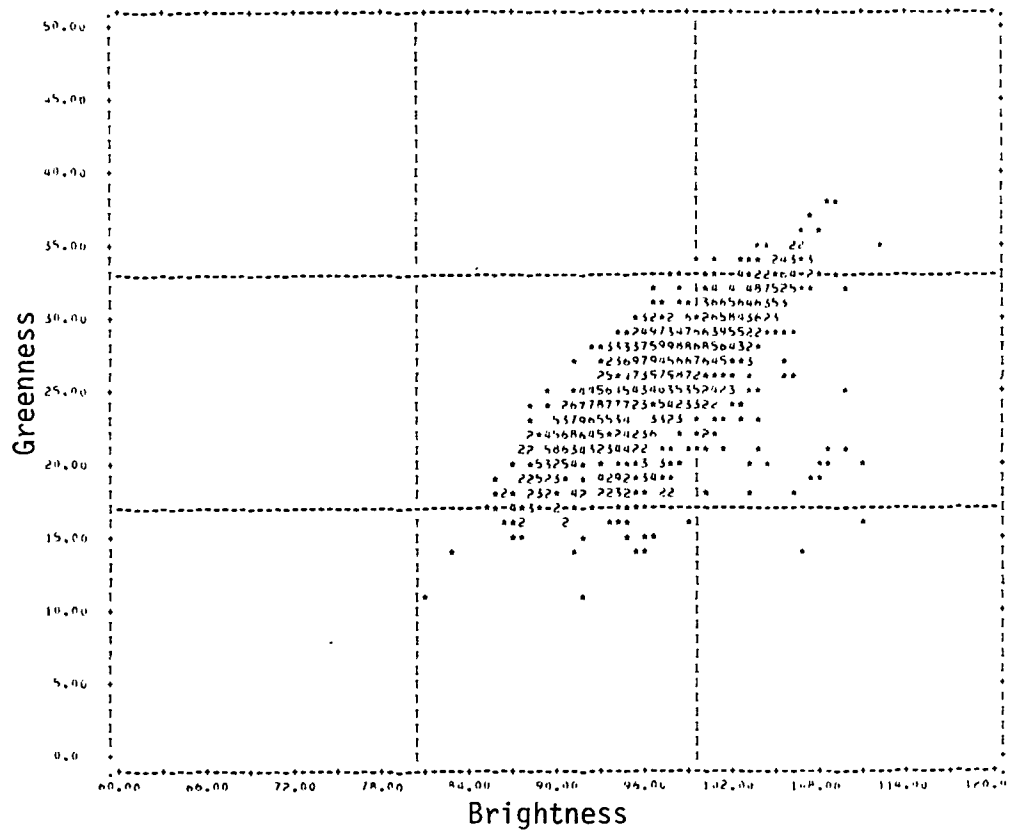


(b) Pure Soybeans Pixels

FIGURE 7. CORN VS. SOYBEANS FOR DAY 178



(a) Pure Corn Pixels



(b) Pure Soybeans Pixels

FIGURE 8. CORN VS. SOYBEANS FOR DAY 205

Figures 9(a) and 9(b) give the Greenness/Brightness scatterplots for pure corn and soybean pixels respectively at day of year 223. This is the date that the expected corn/soybeans separation occurs in this simulation. Soybeans are now at their peak green value. The decision line $G = -.62B + 11.32$ allows about 90% correct classification of corn and soybeans at the pixel level and about 98% at the field level.

Figures 10, 11, 12, and 13 give Greenness/Brightness images for the same dates.

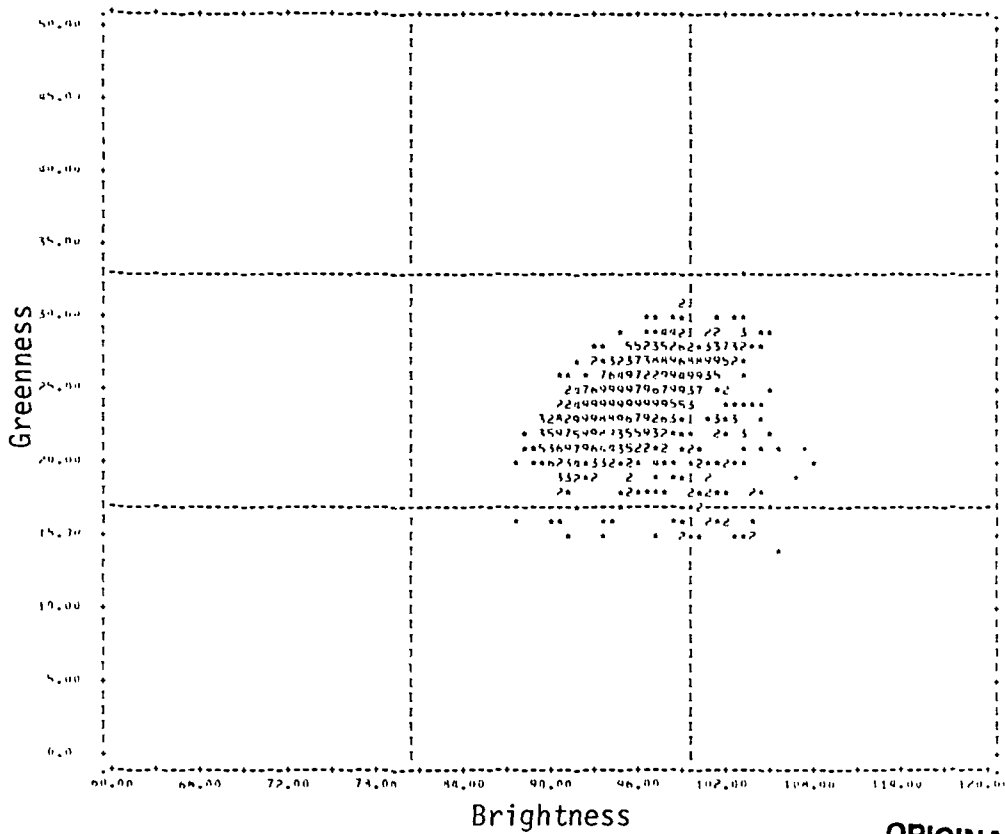
In Figure 10 (Day 160) summer crops can be separated from grain pasture, sunflowers, and flax. The summer crops are very dark on the image for this date.

In Figure 11 (Day 178) summer crops are greening up with most corn fields displaying a higher Greenness value than soybean fields. Pasture and sunflowers still have a fairly high Greenness value. The flax fields are very dark in this image. The grain fields have a low Greenness value and a high Brightness value which shows up as a light blue on this image.

In Figure 12 (Day 205) soybeans generally have a higher Greenness value than corn but many soybean fields have not separated from corn which would give a biased proportion estimate in favor of corn. The pasture fields have greened down and now look a lot like the grain fields. The sunflowers still display a detectable Greenness value.

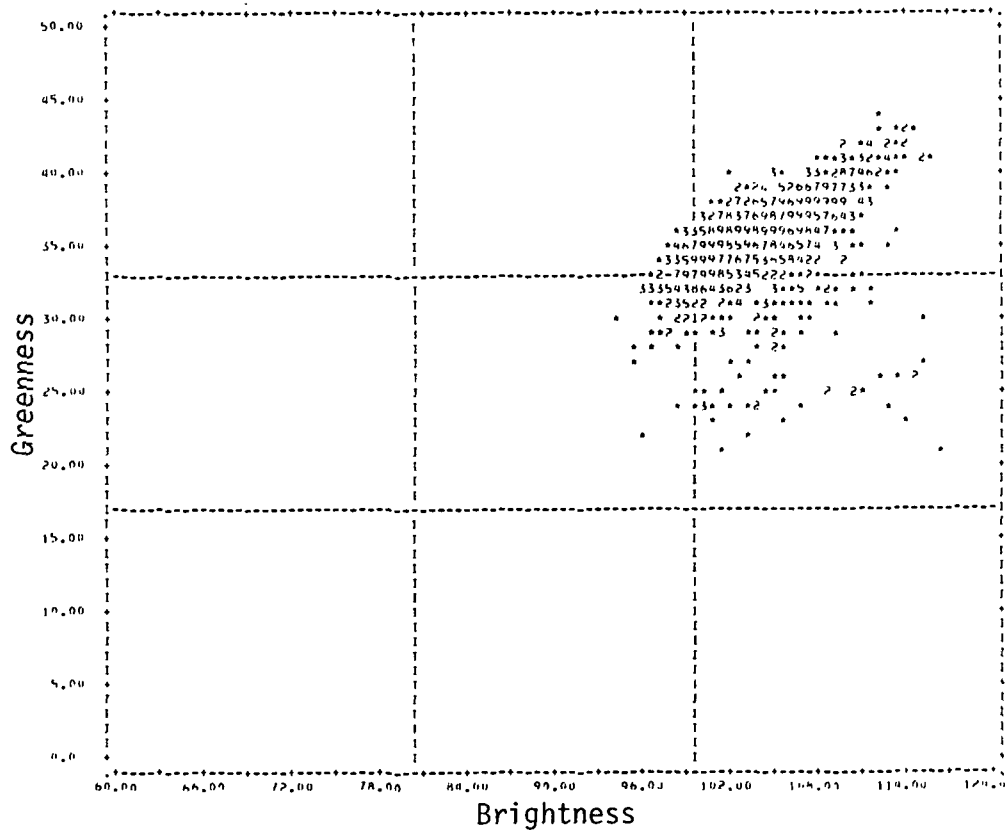
In Figure 13 (Day 223) almost all of the soybean fields have a higher Greenness value than corn fields. The soybean fields appear as bright yellow/orange while the corn fields appear as a dark brown/orange.

Fields can be detected for the most part when all four dates are used, the Date 160 provides perfect summer crop/non-summer crop separation, and the Date 223 provides nearly perfect corn/soybeans separation.



(a) Pure Corn Pixels

**ORIGINAL PAGE IS
OF POOR QUALITY**



(b) Pure Soybeans Pixels

FIGURE 9. CORN VS. SOYBEANS FOR DAY 223

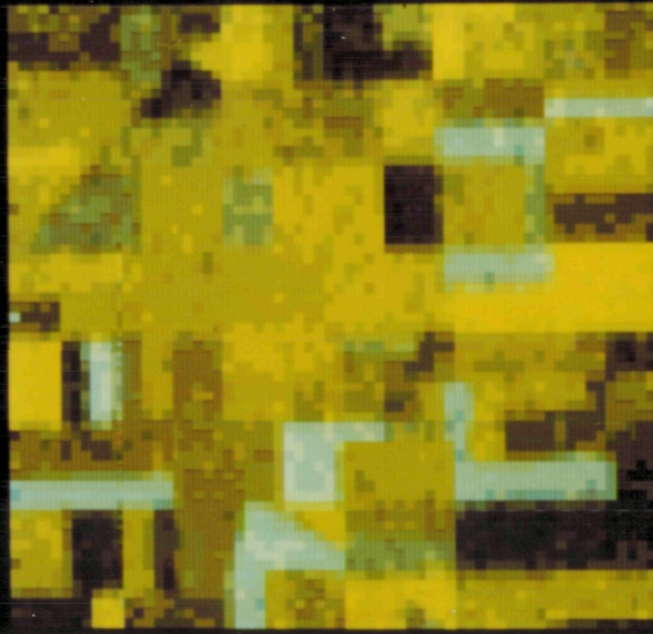


FIGURE 10. SIMULATED IMAGE FOR DAY 160

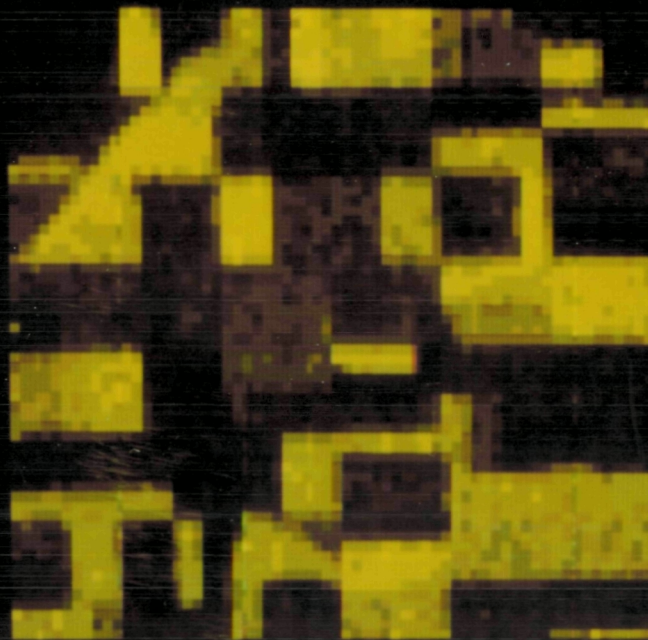


FIGURE 11. SIMULATED IMAGE FOR DAY 178

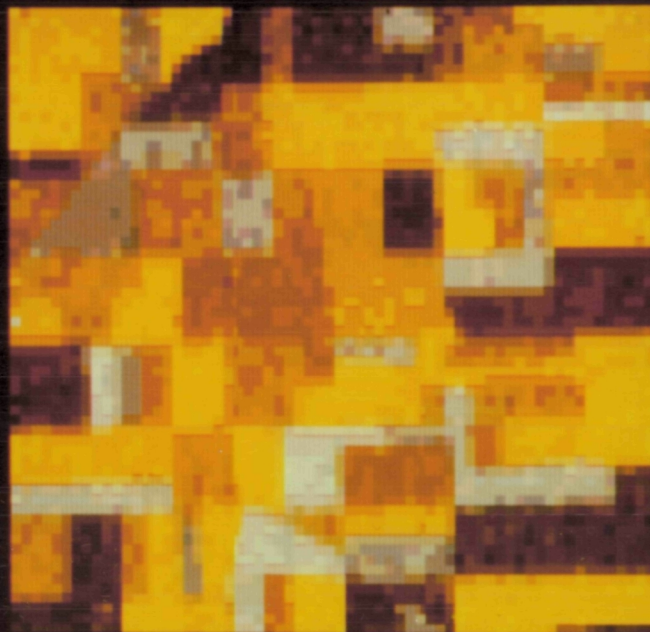


FIGURE 12. SIMULATED IMAGE FOR DAY 205

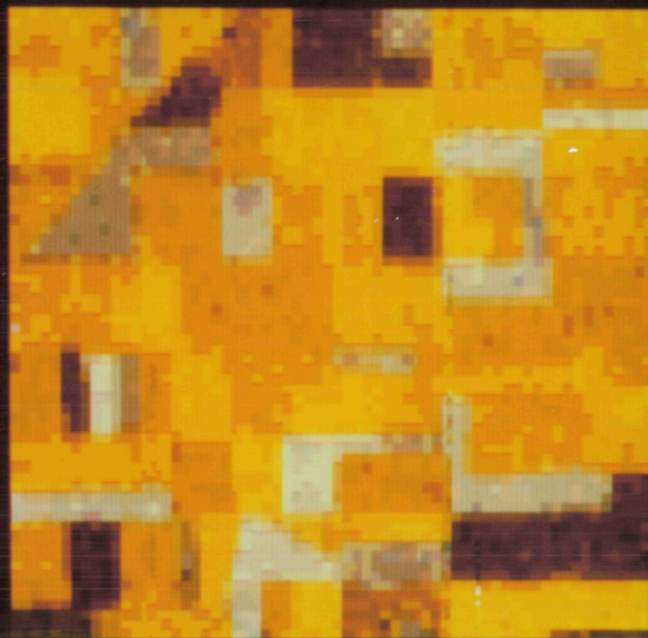


FIGURE 13. SIMULATED IMAGE FOR DAY 223



5

SUMMARY

The present understanding of several components in the Landsat signal-generation process allows the simulation of Landsat data. The simulation described in this report allows for:

- (1) Mixed pixels,
- (2) Field geometry,
- (3) Landsat point spread function,
- (4) Crop development spectral profiles,
- (5) Variation in planting dates,
- (6) Within-field variation, and
- (7) Misregistration.

The simulation has been used in small field research. Other applications include the simulation of other sensors, the test of new procedures, and the study of new crop mixes and field patterns.

REFERENCES

1. Crist, E. P. and W. A. Malila, Development and Evaluation of an Automatic Labeling Technique for Spring Small Grains, Environmental Research Institute of Michigan, Ann Arbor, Michigan, Report No. SR-EI-04065, June 1981.
2. Dye, R. H., Restoration of Landsat Images by Discrete Two-Dimensional Deconvolution, presented at the Proceedings of the Tenth International Symposium on Remote Sensing of Environment, Ann Arbor, Michigan, October 1975.
3. Wilson, C. L., Landsat Derived Maps of Poorly Mapped Areas, presented at the Third Annual International Users' Conference on Computer Mapping Hardware, Software and Data Bases, Cambridge, Massachusetts, July 1980.

PRECEDING PAGE BLANK NOT FILMED



DISTRIBUTION LIST

<u>Name</u>	<u>Number of Copies</u>
NASA/Johnson Space Center Earth Resources Research Division Houston, Texas 77058	
Attn: Dr. G. Badhwar/SG3	1
Attn: Mr. I. D. Browne/SG3	2
Attn: Dr. J. W. Dietrich/SG3	1
Attn: Dr. A. H. Feiveson/SG3	1
Attn: Dr. F. G. Hall/SG3	1
Attn: Mr. D. Hay/SG2	1
Attn: Dr. R. P. Heydorn/SG3	1
Attn: Dr. A. G. Houston/SG3	1
Attn: Mr. R. B. MacDonald/SG	1
Attn: Dr. D. E. Pitts/SG3	1
Attn: Dr. M. L. Steib/SG3	1
Attn: Dr. D. Thompson/SG3	1
Attn: CASPAN Library/SG	2
Attn: Mr. T. C. Minter/C09	4

NASA/Johnson Space Center
Earth Resources Applications Division
Houston, Texas 77058

Attn: Mr. K. Baker/SH3	1
Attn: Mr. R. M. Bizzell/SH3	1
Attn: Mr. J. L. Dragg/SH3	1
Attn: Dr. J. D. Erickson/SH	1
Attn: Dr. D. L. Henninger/SH3	1
Attn: Mr. F. J. Herbert/SH3	1
Attn: Mr. W. C. Jones/SH3	1
Attn: Mr. R. McKinney/SH3	1
Attn: Mr. T. W. Pendleton/SH2	1
Attn: Mr. H. L. Prior/SH3	1
Attn: Mr. M. C. Trichel/SH2	1
Attn: Mr. L. C. Wade/SH3	2
Attn: Dr. V. S. Whitehead/SH3	1
Attn: Dr. B. L. Carroll/C09	4



DISTRIBUTION LIST (Continued)

<u>Name</u>	<u>Number of Copies</u>
NASA/Johnson Space Center Technical Library Branch Houston, Texas 77058 Attn: Mr. M. P. McDonough/JM6	4
NASA/Johnson Space Center Technical Support Procurement Branch Houston, Texas 77058 Attn: Ms. E. McAnelly/BB63	1
NASA/Johnson Space Center Space and Life Sciences Directorate Houston, Texas 77058 Attn: Mr. W. E. Rice	1
NASA/Johnson Space Center NOAA Liaison Office Houston, Texas 77058 Attn: Mr. M. Helfert/SK	1
NASA/Ames Research Center Moffett Field, California 94035 Attn: Dr. D. M. Deerwester	1
NASA/Goddard Space Flight Center Greenbelt, Maryland 20771 Attn: Dr. J. Barker/923 Attn: Mr. W. Alford/563 Attn: Mr. F. Gordon/902	1 1 1
NASA Headquarters Washington, D.C. 20546 Attn: Mr. Howard Hogg/ER-2 Attn: Mr. James Welch/ER-2	1 1



DISTRIBUTION LIST (Continued)

<u>Name</u>	<u>Number of Copies</u>
NASA/Goddard Institute for Space Studies New York, New York 10025 Attn: Dr. S. G. Unger	1
Agency for International Development Office of Science and Technology/SA-18 Washington, D.C. 20523 Attn: Dr. C. K. Paul	1
Colorado State University College of Forestry and Natural Resources Fort Collins, Colorado 80523 Attn: Dr. J. Smith	1
Earth Resources Laboratory National Space Technology Laboratory Bay St. Louis, Mississippi 39520 Attn: Dr. D. W. Mooneyhan	1
EROS Data Center U.S. Department of Interior Sioux Falls, South Dakota 57198 Attn: Mr. G. Thorley Attn: Mr. A. Watkins	1 1
Environmental Protection Agency Western Environmental Research Laboratories P.O. Box 15027 Las Vegas, Nevada 89114 Attn: Chief of Technical Support	1
General Electric Company Space Division 4701 Forbes Blvd. Lanham, Maryland 20801 Attn: Dr. A. B. Park	1



DISTRIBUTION LIST (Continued)

<u>Name</u>	<u>Number of Copies</u>
NOAA Chief, Climatic Impact Assessment Division 3300 Whitehaven, NW Page Bldg. 2, Rm. 140 Washington, D.C. 20250 Attn: Dr. Russell A. Ambrosiak	1
NOAA/NESS Office of Research Department of Commerce Washington, D.C. 20233 Attn: Dr. Harold Yates	1
NOAA/Code OAX-1 Environmental Data and Information Services Washington, D.C. 20235 Attn: Dr. Thomas Potter	1
NOAA CEAS Federal Building Columbia, Missouri 65201 Attn: Dr. W. Wilson	1
North Dakota State University Plant Pathology Department Fargo, North Dakota 58102 Attn: Dr. V. Pederson	1
Oregon State University Environmental Remote Sensing Applications Laboratory Corvallis, Oregon 97331 Attn: Dr. Barry J. Schrupf	1



DISTRIBUTION LIST (Continued)

<u>Name</u>	<u>Number of Copies</u>
Pennsylvania State University Office for Remote Sensing of Earth Resources 112 ABL Building University Park, Pennsylvania 16802 Attn: Dr. Gary W. Peterson	1
Prairie View A&M University College of Agriculture Prairie View, Texas 77445 Attn: Dr. E. Brams	1
Purdue University Purdue Industrial Research Park 1220 Potter Drive West Lafayette, Indiana 47906 Attn: Dr. Marvin Bauer	3
South Dakota State University Remote Sensing Institute Box 507 Brookings, South Dakota 57007 Attn: Mr. Victor I. Myers Attn: Dr. J. C. Harlan	1 1
Texas A&M University Department of Mathematics College Station, Texas 77843 Attn: Dr. L. F. Guseman, Jr.	1
U.S. Department of Agriculture Grassland, Soil & Water Research Laboratory P.O. Box 748 Temple, Texas 76501 Attn: Dr. J. T. Ritchie	1



DISTRIBUTION LIST (Continued)

<u>Name</u>	<u>Number of Copies</u>
Texas A&M University Remote Sensing Center Teague Building College Station, Texas 77843 Attn: Dr. James Heilman	1
U.S. Department of Agriculture SEA/AR Bldg. 005, Rm. 125 BARC-West Beltsville, Maryland 20705 Attn: Mr. Carl W. Carlson	1
U.S. Department of Agriculture SEA/NPS Bldg. 005, Rm. 233A BARC-West Beltsville, Maryland 20705 Attn: Mr. Jerry Ritchie	1
U.S. Department of Agriculture Forest Service 240 W. Prospect Street Fort Collins, Colorado 80521 Attn: Dr. Richard Driscoll	1
U.S. Department of Agriculture FAS-CCAD 1050 Bay Area Blvd. Houston, Texas 77058 Attn: Mr. James Hickman	2
U.S. Department of Agriculture AgRISTARS/EW 1050 Bay Area Blvd. Houston, Texas 77058 Attn: Dr. G. O. Boatwright	1

DISTRIBUTION LIST (Continued)

<u>Name</u>	<u>Number of Copies</u>
U.S. Department of Agriculture Economics and Statistics Service Washington, D.C. 20250	
Attn: Mr. Rich Allen	1
Attn: Mr. Charles E. Caudill	1
Attn: Mr. Galen F. Hart	1
Attn: Mr. William E. Kibler	1
U.S. Department of Agriculture/SCS 1943 Newton Square East Reston, Virginia 22090	
Attn: Dr. R. H. Gilbert	1
U.S. Department of Agriculture Soil & Water Conservation Research Division P.O. Box 267 Weslaco, Texas 78596	
Attn: Dr. Craig Wiegand	1
U.S. Department of Interior Geological Survey 1925 Newton Square East Reston, Virginia 22070	
Attn: Mr. Fred Doyle	1
U.S. Department of Interior Geological Survey Federal Center Denver, Colorado 80225	
Attn: Dr. Harry W. Smedes	1
University of Arkansas Mathematics Department Fayetteville, Arkansas 72704	
Attn: Dr. Jack D. Tubbs	1



DISTRIBUTION LIST (Continued)

<u>Name</u>	<u>Number of Copies</u>
University of California at Berkeley Forestry Department Berkeley, California 94720 Attn: Mr. Robert Colwell	1
University of California t Berkeley 260 Space Sciences Laboratory Berkeley, California 94720 Attn: Ms. Claire M. Hay	3
University of Nebraska Agricultural Meteorology Section 211 Agricultural Engineering Lincoln, Nebraska 68583 Attn: Dr. B. L. Blad	1
University of Texas at Dallas Box 688 Richardson, Texas 75080 Attn: Dr. Patrick L. Odell	1
University of Tulsa Mathematics-Sciences Department 600 South College Tulsa, Oklahoma 74104 Attn: Dr. W. A. Coberly	1
Kansas State University Evapotraspiration Laboratory Manhattan, Kansas 66506 Attn: Dr. Edward T. Kanemasu	1
University of California Department of Geography Santa Barbara, California 93106 Attn: Dr. John E. Estes	1

DISTRIBUTION LIST (Continued)

<u>Name</u>	<u>Number of Copies</u>
U.S. Department of Agriculture Forest Service/NFAP 1050 Bay Area Blvd. Houston, Texas 77058 Attn: Dr. F. P. Weber	1
NASA/Johnson Space Center Houston, Texas 77058 Attn: Mr. Fred Barrett Mail Code SK/USDA	3